



# True-amplitude CRS-based Kirchhoff time migration for AVO analysis

Miriam Spinner and Jürgen Mann, Geophysical Institute, University of Karlsruhe, Germany

Copyright 2005, SBGf – Sociedade Brasileira de Geofísica

This paper was prepared for presentation at the 9<sup>th</sup> International Congress of The Brazilian Geophysical Society held in Salvador, Brazil, September 11-14 2005.

Contents of this paper was reviewed by The Technical Committee of the 9<sup>th</sup> International Congress of The Brazilian Geophysical Society and does not necessarily represent any position of the SBGf, its officers or members. Electronic reproduction, or storage of any part of this paper for commercial purposes without the written consent of The Brazilian Geophysical Society is prohibited.

## Summary

The achievable image quality and the reliability of amplitudes in Kirchhoff migration strongly depend on the selection of the migration aperture. Too small an aperture leads to underestimated amplitudes and the loss of steep events. On the other hand, too large apertures tend to cause operator aliasing and include unnecessary noise and contributions from unwanted events. Our aim is to use CRS-based minimum apertures in Kirchhoff prestack time migration to obtain the best possible input for AVO/AVA analyses.

The basic idea is demonstrated for a synthetic data set which contains events from a common sequence of gas/water/oil contacts. We discuss the determination and extrapolation of stationary points and projected Fresnel zones based on CRS wavefield attributes, as well as a simple and efficient way to set up a migration velocity model. The first results show a significant reduction of amplitude dispersion in common-image gathers as well as in the zero-offset section, thus providing superior input to AVO/AVA analyses.

## Introduction

The Common-Reflection-Surface (CRS) stack method as highly automated imaging process has been successfully applied to various data sets. Its implementation for zero-offset (ZO) simulation was initially mainly considered as an alternative to stacking procedures like normal moveout/dip moveout(NMO/DMO)/stack. Meanwhile, the stacking parameters of the CRS stack, the so-called kinematic wavefield attributes, turned out to be extremely useful for various purposes: estimation of projected Fresnel zones and geometrical spreading factors, tomographic velocity model determination, etc.

CRS stack, tomographic velocity model determination, and true-amplitude Kirchhoff migration have been combined to set up a consistent CRS-based imaging workflow from the prestack data to the depth migrated image (Hertweck et al., 2003). For optimum amplitude behavior in the migrated image, Kirchhoff migration should be restricted to the projected Fresnel zone, only (Schleicher et al., 1997). Jäger (2005) employed the CRS attributes in pre- and poststack Kirchhoff depth migration to estimate the size and location of this minimum aperture. His primary aim was to reduce migration artifacts and to avoid operator aliasing, but it is

well known that also amplitude-versus-offset (AVO) analysis benefits from amplitudes calculated in the minimum aperture (Bancroft and Sun, 2003).

The advantages of minimum-aperture migration with respect to the amplitude behavior are obvious from Figure 1: in conventional migration (Figure 1a) the stationary point where the operator is tangent to the event and the projected Fresnel zone are unknown prior to migration. Thus, the aperture has to be centered around the operator's apex and has to be chosen sufficiently large to preserve steep events. As a consequence, a lot of noise off the event and possibly other events contribute to the stack and deteriorate the amplitudes. In addition, the risk of operator aliasing is increased. In contrast, the minimum-aperture operator (Figure 1b) avoids these problems as its location and size fits the constructively contributing part of the reflection event.

Pruessmann et al. (2004) presented a first approach to perform CRS-based AVO analysis in the *unmigrated* time domain. For complex media, a migration prior to AVO analysis might, however, be inevitable. As depth migration is quite sensitive to velocity model errors and costly in terms of inversion, we propose the happy medium: CRS-based AVO analysis in the *migrated* time domain. There, we benefit from

- reduced sensitivity to model errors,
- simple and largely automated model building,
- smooth, analytic migration operators and operator slopes, and
- consistent, analytic approximation of true-amplitude weight factors.

## Basics of CRS stack

The CRS method is based on a second-order approximation of the kinematic reflection response of an arbitrarily curved reflector segment in depth. This approximation can be entirely expressed in terms of so-called kinematic wavefield attributes defined at the acquisition surface rather than in the subsurface. In 2D, the commonly used hyperbolic approximation reads (see, e.g., Schleicher et al., 1993):

$$t^2(x_m, h) = \left[ t_0 + \frac{2 \sin \alpha (x_m - x_0)}{v_0} \right]^2 + \frac{2 t_0 \cos^2 \alpha}{v_0} \left[ \frac{(x_m - x_0)^2}{R_N} + \frac{h^2}{R_{NIP}} \right]. \quad (1)$$

It describes the traveltimes along a paraxial ray characterized by source/receiver midpoint  $x_m$  and half-offset  $h$

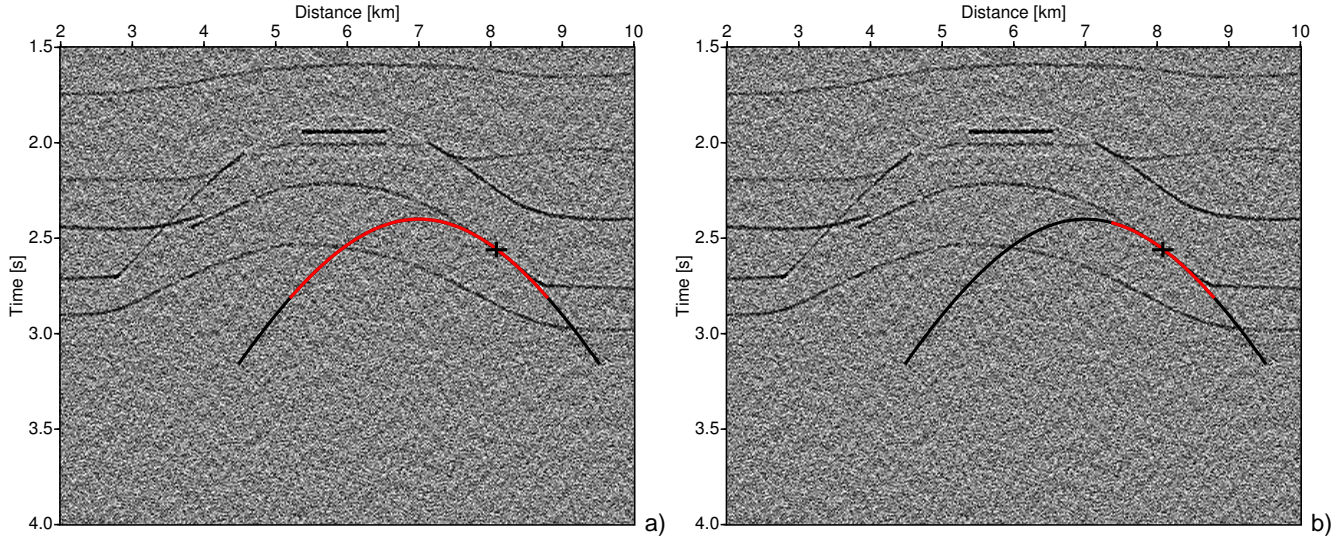


Figure 1: Time migration operator with a) conventional aperture centered around its apex and with b) minimum aperture centered around stationary point. The respective part of the operator within the aperture is depicted in red.

in terms of the traveltimes  $t_0$  along the central normal ray emerging at  $x_0$ , the near-surface velocity  $v_0$ , and the wavefield attributes  $\alpha$ ,  $R_{\text{NIP}}$ , and  $R_{\text{N}}$ . The latter three are related to the propagation direction and wavefront curvatures of two hypothetical waves, namely the so-called NIP and normal wave, respectively (Hubral, 1983).

Similar to a conventional stacking velocity analysis, the optimum wavefield attributes for each location  $(x_0, t_0)$  are determined automatically by means of coherence analysis. Note, however, that this analysis is carried out with a spatial operator in a multi-dimensional parameter domain. The final results are entire sections of the wavefield attributes  $\alpha$ ,  $R_{\text{NIP}}$ , and  $R_{\text{N}}$ , as well as coherence section. For details we refer, e. g., to Jäger et al. (2001).

### Determination of stationary points

In Kirchhoff migration, the main contribution to the diffraction stack stems from the region where the reflection event is tangent to the migration operator. As the CRS operator (1) is already tangent to a reflection event in the data, this tangency condition can be directly evaluated by a comparison of CRS operator slope and migration operator slope. This is particularly easy for the ZO case where the CRS operator simplifies. In case of Kirchhoff depth migration, the migration operator slope has to be calculated numerically from the Greens function tables (Jäger, 2005). For time migration with straight rays as considered here, the operator as well as its derivatives are given by analytic expressions.

In practice, we calculate the modulus of the difference between these two slopes and choose the location of the minimum as stationary point. The associated coherence values help to decide whether the stationary point is reliable or not by applying a user-given threshold.

### Estimation of minimum aperture

By definition, the point  $(x_0, t_0)$  in operator (1) is the stationary point for ZO in the context of Kirchhoff migration. The

concept of the *Common-Reflection-Point (CRP) trajectory* allows to extrapolate this stationary point to finite offset. Its projection onto the acquisition surface reads (Höcht et al., 1999):

$$x_m(h) = x_0 + r_T \left( \sqrt{\frac{h^2}{r_T^2} + 1} - 1 \right), \quad (2a)$$

with

$$r_T = \frac{R_{\text{NIP}}}{2 \sin \alpha}. \quad (2b)$$

The final information relevant for minimum migration apertures which can be gained from the attributes is the size of the projected ZO Fresnel zone  $W_F$ . In terms of CRS attributes, it can be approximated as (see, e. g., Mann, 2002)

$$\frac{W_F}{2} = |x_m - x_0| = \frac{1}{\cos \alpha} \sqrt{\frac{v_0 T}{2 \left| \frac{1}{R_{\text{N}}} - \frac{1}{R_{\text{NIP}}} \right|}}, \quad (3)$$

where  $T$  denotes some measure of the wavelet length. Unfortunately, an extrapolation of the ZO Fresnel zone to finite offset is not supported by the attributes alone, but requires additional assumptions. For the data example below, we simply used a constant extrapolation to finite offset, an approximation which appears to be reasonably accurate to obtain reliable amplitudes.

### Model determination

The wavefield attributes are attached to the stationary point for ZO, i. e.,  $P_0 = (x_0, t_0)$ . Kirchhoff time migration, however, is usually parameterized in terms of RMS velocities defined at the operator apex.

As the NIP wave does not depend on the reflector curvature and orientation, it allows to approximate the ZO diffraction response of a diffractor located on the (unknown) reflector segment in depth. In this case,  $R_{\text{N}} := R_{\text{NIP}}$ , as normal and

NIP wave coincide:

$$t_D^2(x_m, h) = \left[ t_0 + \frac{2 \sin \alpha (x_m - x_0)}{v_0} \right]^2 + \frac{2 t_0 \cos^2 \alpha}{v_0 R_{\text{NIP}}} \left[ (x_m - x_0)^2 + h^2 \right]. \quad (4)$$

This approximate diffraction response coincides with the optimum poststack time migration operator using the straight ray assumption. Its apex location can be written as (Mann, 2002):

$$x_{\text{apex}} = x_0 - \frac{R_{\text{NIP}} t_0 v_0 \sin \alpha}{2 R_{\text{NIP}} \sin^2 \alpha + t_0 v_0 \cos^2 \alpha}, \quad (5a)$$

$$t_{\text{apex}}^2 = \frac{t_0^3 v_0 \cos^2 \alpha}{2 R_{\text{NIP}} \sin^2 \alpha + t_0 v_0 \cos^2 \alpha}. \quad (5b)$$

In principle, this relation allows to directly migrate a ZO sample by mapping its amplitude to the apex location associated with the ZO location—without any migration velocity model (Mann et al., 2000). By introducing offset bins during the stack along the CRS operator (1), this approach can be extended to the prestack case. However, such a point-to-point mapping does not necessarily provide contiguous images of the reflection events. An interpretation of amplitudes is almost impossible under such conditions, therefore we use the diffraction response to derive a migration velocity model in a conventional sense.

Expressing the CRS diffraction response (4) in apex coordinates (5) immediately yields the familiar poststack time migration operator parameterized with a migration velocity  $v_c$  in terms of CRS wavefield attributes:

$$t_D^2(x) = t_{\text{apex}}^2 + \frac{4(x - x_{\text{apex}})^2}{v_c^2} \quad \text{with} \quad (6a)$$

$$v_c^2 = \frac{2 v_0^2 R_{\text{NIP}}}{2 R_{\text{NIP}} \sin^2 \alpha + v_0 t_0 \cos^2 \alpha}. \quad (6b)$$

For illustration, the approximate diffraction and reflection traveltimes as well as their forward-calculated counterparts are displayed in Figure 2 for a simple model.

Each set of (reliable) CRS attributes can now be related to a migration velocity value and its corresponding location in the time domain. To end up with a smooth velocity model covering the whole target zone, these values have firstly been smoothed along the reflection events in an event-consistent manner (Mann and Duveneck, 2004). In a subsequent infill procedure, the migration velocities are inter- and extrapolated using a distance weighted polynomial interpolation. This approach has, so far, no sound physical justification.

### Synthetic data example

To demonstrate the potential of the true-amplitude CRS-based Kirchhoff time migration for AVO analysis we generated a synthetic prestack data set for the model shown in Figure 3a. The target region for the amplitude extraction is the horizontally layered structure beneath the uppermost dome-like interface. The elastic parameters are chosen such as to mimic a sequence of gas/oil/water contacts. The primary P-waves have been modeled by means of a wavefront construction method using a zero-phase Ricker

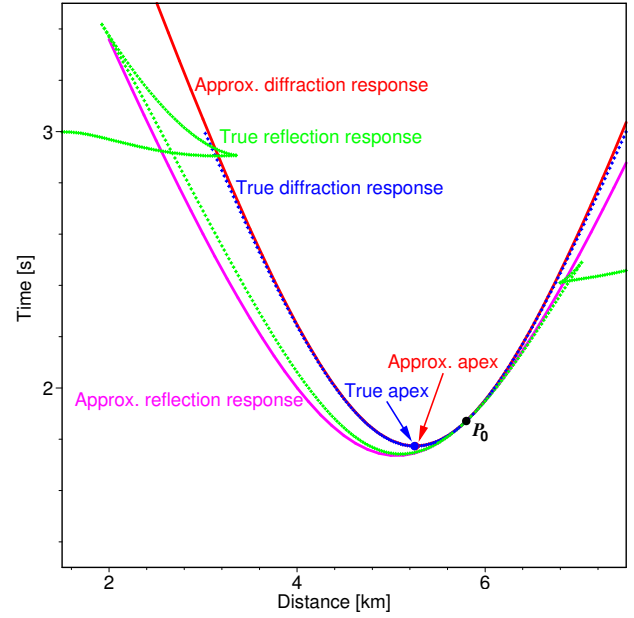


Figure 2: True and approximated ZO reflection and diffraction traveltime curves for a simple layered model. The time migration velocity  $v_c$  is defined at the approximated apex location (red dot) and can be calculated from the CRS wavefield attributes defined at ZO location  $P_0$ . (Figure taken from Mann, 2002)

wavelet with a dominant frequency of 20 Hz. Edge diffractions have not been considered. Colored noise was added; a representative common-offset section is shown in Figure 4.

The CRS stack has been applied to simulate a ZO section (not displayed) in a fully automated way. More relevant in this context are the CRS wavefield attribute sections and the associated coherence section (also not displayed). Based on the coherence values which indicate the location of the reflection events and the reliability of their wavefield attributes, an automated picking process was employed to extract the wavefield attributes along the reflection events. These attributes have been used

- to determine the stationary points for ZO,
- to extrapolate the stationary points to finite offset,
- to estimate the projected ZO Fresnel zone, and
- to calculate time-migration velocity values.

The interpolated smooth time-migration velocity model shown in Figure 3b is based on these velocity values. The model is kinematically consistent with the data as can be seen from the set of common-image gathers (CIGs) displayed in Figure 5.

The time migration was performed twice: on the one hand in a conventional way with user-given aperture, on the other hand with the minimum aperture given by the (extrapolated) projected Fresnel zone. The user-given aperture was

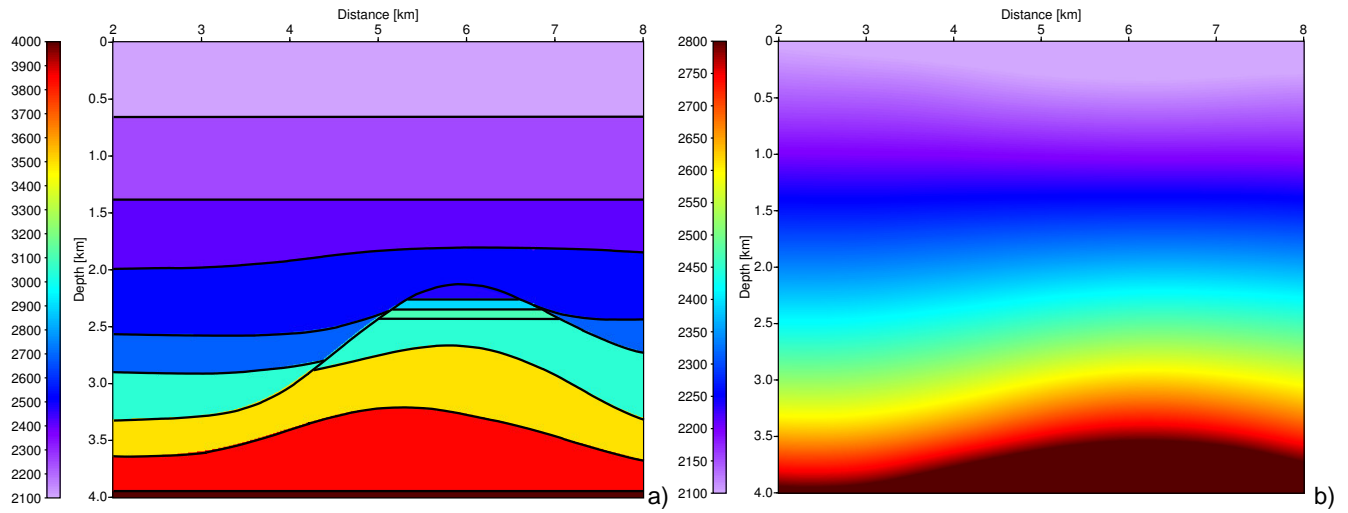


Figure 3: a) Interval P-wave velocity model used to generate the synthetic data, b) time migration velocity model determined from CRS wavefield attributes. Note the different color scales.

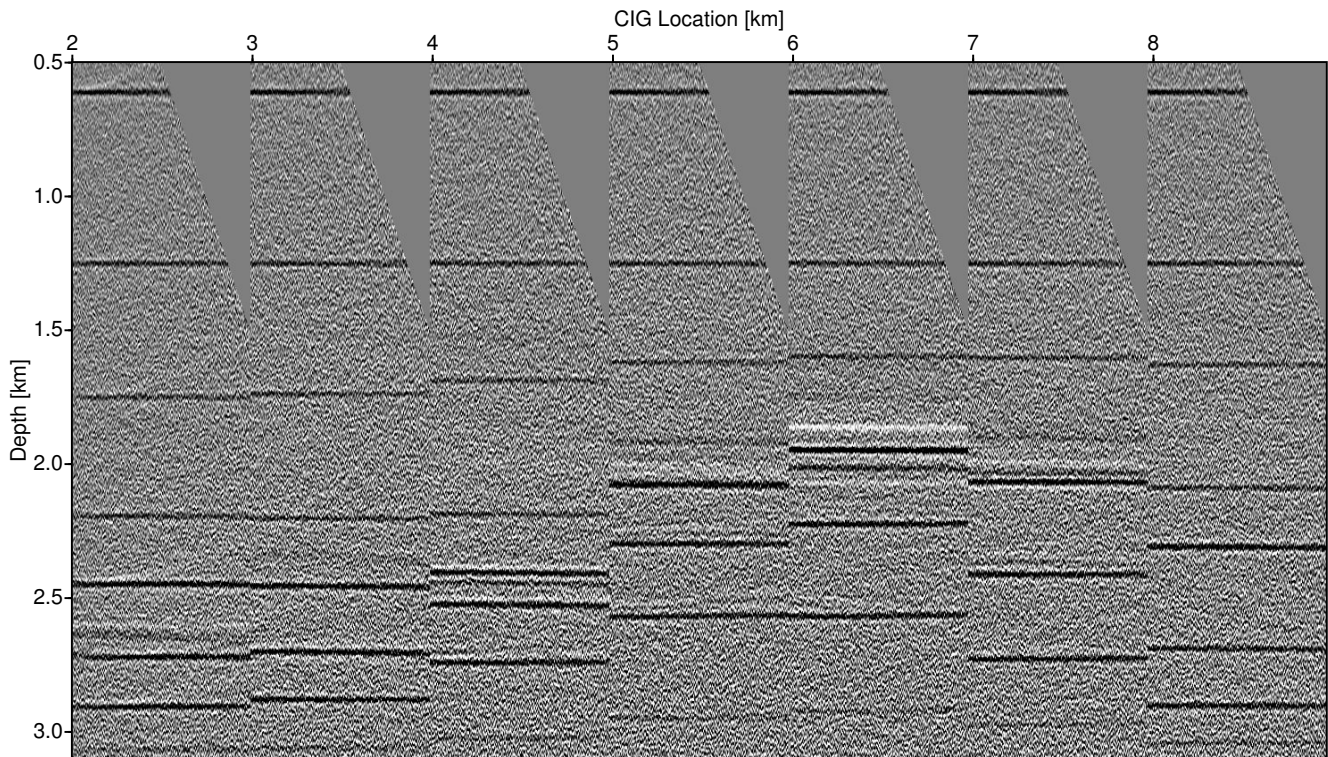


Figure 5: Several common-image gathers extracted from the time-migrated prestack data.

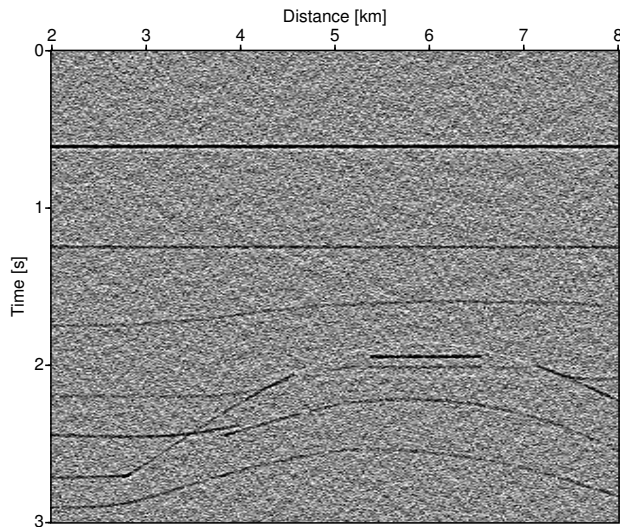


Figure 4: Representative common-offset section ( $h = 100$  m) extracted from the synthetic prestack data.

chosen such that the steep flanks of the dome-like structure has been imaged. The projected ZO Fresnel zone is shown in Figure 6 for those locations where stationary points have been detected. As expected, its size increases with increasing traveltimes and increasing curvature of the reflection events.

Stacks of the two true-amplitude prestack migration results are depicted in Figure 7. For Figure 7b, the minimum-aperture migration was only performed at locations where stationary points have been detected. This removes many of the artifacts due to modeling deficiencies, but might cause gaps in the events, weak events (e. g. the lowermost event) might be entirely lost. In practice, we use the user-given aperture at all other locations to obtain a fully covered image without gaps. The current implementation does not yet guarantee a smooth transition between these two aperture definitions and might, thus, locally introduce some artifacts in the amplitudes.

Finally, we extracted the amplitudes along the images of the target reflectors. Figure 8 shows the amplitude along the uppermost target reflector (directly beneath the dome-like interface) for one of the CIGs (Figure 8a) and for offset zero (Figure 8b). The amplitudes are shown for both aperture definitions applied to the noisy data. In addition, the minimum-aperture migration has been applied to the same data without noise to obtain reference values. Obviously, the CRS-based results are closer to the reference values and far more contiguous compared to their conventional counterparts. Thus, they provide superior input to any kind of AVO/AVA analysis.

## Conclusions

Jäger (2005) successfully applied CRS wavefield attributes to estimate the location of stationary points and the projected Fresnel zone required for minimum-aperture Kirchhoff depth migration. We demonstrated that this CRS-based minimum aperture concept can be transferred back to the time domain. In the time domain, not only the sensitivity to model errors is reduced, but the time migration

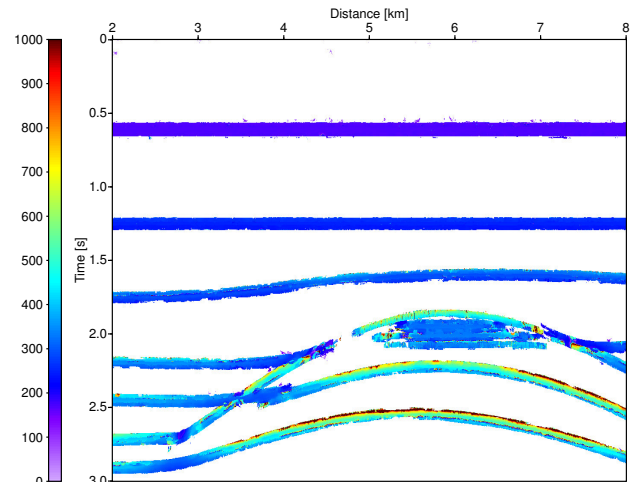


Figure 6: Size of projected first ZO Fresnel zone estimated from the CRS attributes. Only locations with identified stationary points have been considered.

velocity model building can be performed in a highly automated and simple way. The entirely analytic migration operators and their corresponding derivatives allow an efficient implementation, especially concerning the determination of stationary points.

Due to the reduced sensitivity to model errors and the optimum migration aperture we obtain more reliable amplitudes for AVO/AVA analyses compared to conventional approaches.

## Outlook

As future improvement, a physically sound model infill procedure should be incorporated. Furthermore, the extrapolation of the projected Fresnel zone to finite offset has to be investigated in more detail. In case the migration is performed at all image locations rather than at locations with detected stationary points, only, a consistent smoothing of the projected Fresnel zone into the remaining areas with user-given aperture should be introduced to avoid artifacts due to the discontinuous aperture size.

## Acknowledgments

We would like to thank the sponsors of the Wave Inversion Technology (WIT) Consortium for their support.

## References

- Bancroft, J. and Sun, S. (2003). Fresnel zones and the power of stacking used in the preparation of data for AVO analysis. In *Expanded abstracts, 73rd Ann. Internat. Mtg.*, pages 231–234. Soc. Expl. Geophys.
- Hertweck, T., Jäger, C., Mann, J., and Duvencq, E. (2003). An integrated data-driven approach to seismic reflection imaging. In *Extended abstracts, 65th Conf. Eur. Assn. Geosci. Eng. Session P004*.
- Höcht, G., de Bazelaire, E., Majer, P., and Hubral, P. (1999). Seismics and optics: hyperbolae and curvatures. *J. Appl. Geoph.*, 42(3,4):261–281.

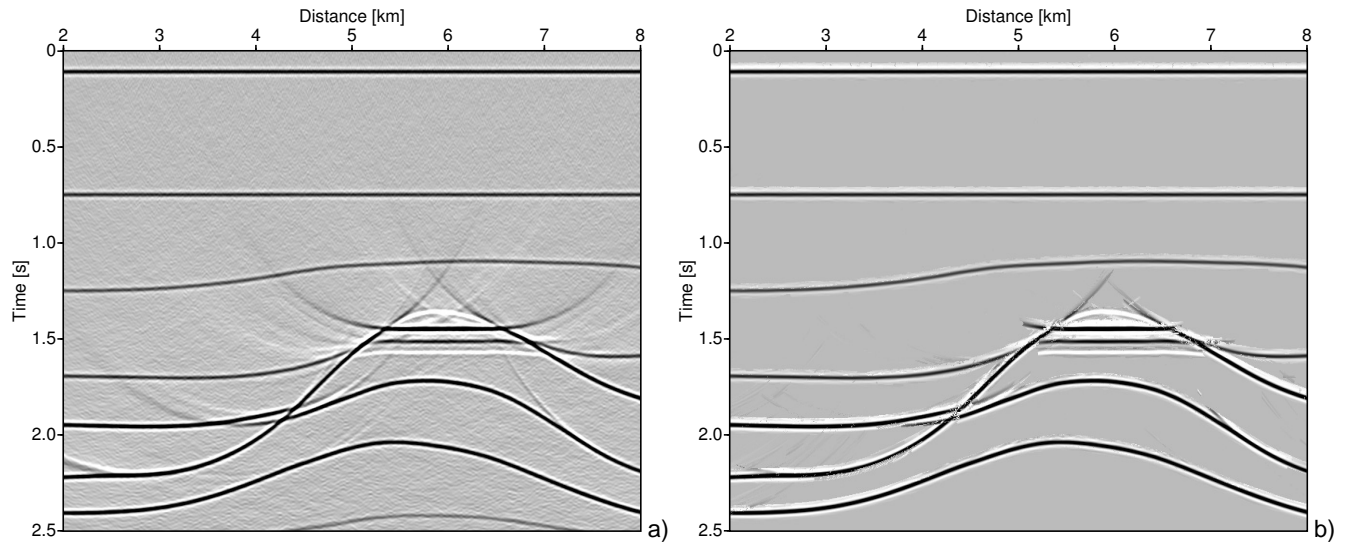


Figure 7: Stacks of the time-migrated prestack data with a) conventional user-defined aperture and b) CRS-based minimum-aperture. In the latter case, only locations with identified stationary points have been considered. The artifacts mainly visible in the conventional result are due to missing edge diffractions and gaps in the modeled prestack data.

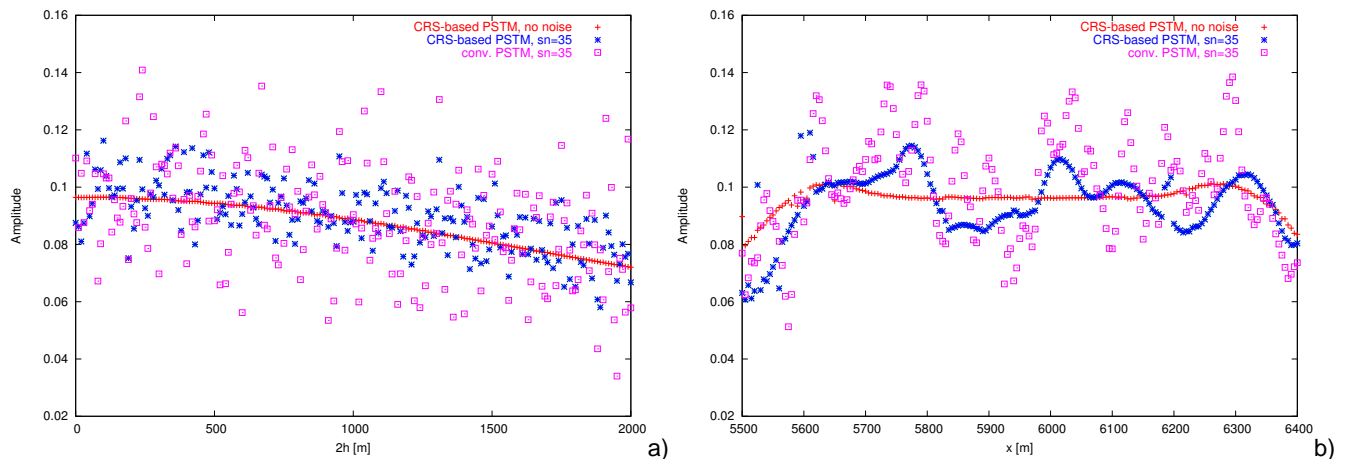


Figure 8: Amplitudes along the first target reflector extracted from the time-migrated prestack data a) for a CIG and b) for ZO. Note the significant differences in dispersion.

Hubral, P. (1983). Computing true amplitude reflections in a laterally inhomogeneous earth. *Geophysics*, 48(8):1051–1062.

Jäger, C. (2005). Minimum-aperture Kirchhoff migration by means of CRS attributes. In *Extended abstracts, 66th Conf. Eur. Assn. Geosci. Eng. Session F042*.

Jäger, R., Mann, J., Höcht, G., and Hubral, P. (2001). Common-Reflection-Surface stack: image and attributes. *Geophysics*, 66(1):97–109.

Mann, J. (2002). *Extensions and applications of the Common-Reflection-Surface Stack method*. Logos Verlag, Berlin.

Mann, J. and Duvencek, E. (2004). Event-consistent smoothing in generalized high-density velocity analysis. In *Expanded Abstracts, 74th Ann. Internat. Mtg. Soc. Expl. Geophys. Session ST 1.1*.

Mann, J., Hubral, P., Traub, B., Gerst, A., and Meyer,

H. (2000). Macro-model independent approximative prestack time migration. In *Extended abstracts, 62nd Conf. Eur. Assn. Geosci. Eng. Session B-52*.

Pruessmann, J., Coman, R., Endres, H., and Trappe, H. (2004). Improved imaging and AVO analysis of a shallow gas reservoir by CRS. *The Leading Edge*, 23(9):915–918.

Schleicher, J., Hubral, P., Tygel, M., and Jaya, M. S. (1997). Minimum apertures and Fresnel zones in migration and demigration. *Geophysics*, 62(1):183–194.

Schleicher, J., Tygel, M., and Hubral, P. (1993). Parabolic and hyperbolic paraxial two-point traveltimes in 3D media. *Geophys. Prosp.*, 41(4):495–514.